



127  
663  
THS



3 1293 01026 9730

This is to certify that the

thesis entitled

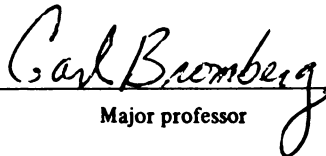
"New Methods in Optical Fiber  
Preparation For Scintillating  
Tile Calorimetry"

presented by

**Benn Harold Tannenbaum**

has been accepted towards fulfillment  
of the requirements for

M.S. degree in Physics

  
Major professor

Date November 16, 1993

**LIBRARY  
Michigan State  
University**

**PLACE IN RETURN BOX to remove this checkout from your record.  
TO AVOID FINES return on or before date due.**

<b>DATE DUE</b>	<b>DATE DUE</b>	<b>DATE DUE</b>
_____	_____	_____
_____	_____	_____
_____	_____	_____
_____	_____	_____
_____	_____	_____
_____	_____	_____
_____	_____	_____

**NEW METHODS IN OPTICAL FIBER  
PREPARATION FOR SCINTILLATING  
TILE CALORIMETRY**

By

**Benn Harold Tannenbaum**

**A THESIS**

Submitted to  
Michigan State University  
in partial fulfillment of the requirements  
for the Degree of

**MASTER OF SCIENCE**

**Department of Physics and Astronomy**

**1993**

## ABSTRACT

### NEW METHODS IN OPTICAL FIBER PREPARATION FOR SCINTILLATING TILE CALORIMETRY

By

Benn Harold Tannenbaum

Michigan State University has developed a semi-automatic splicing machine to weld clear, wavelength shifting and scintillating polystyrene fibers. The splicing technique has been refined to produce splices with an average transmission of 95.7% and a  $\sigma$  of 3.7%. The splicer is easily modified to work with a variety of fiber types and sizes and will be of great value as the use of fibers in calorimetry and tracking increases. Also, a multiple fiber linear scanner has been developed to allow quick and easy feedback on the quality of the spliced fibers. Finally, an  $x-y$  scanner has been developed to examine photocathode response uniformity of photomultiplier tubes and the effectiveness of light mixers.

## ACKNOWLEDGEMENTS

I thank Carl Bromberg and Joey Huston, my advisors, and John Mansour, for all their help, Ron Richards and Sharon Joy for designing and building the splicer, Dean Shooltz for building the  $x$ - $y$  scanner, Ewa Skup and Pam Schmidt for helping splice fibers and collect data and Aleks Kuzminski for helping with the figures.

# Contents

<b>LIST OF TABLES</b>	<b>v</b>
<b>LIST OF FIGURES</b>	<b>vi</b>
<b>1 Introduction</b>	<b>1</b>
<b>2 History</b>	<b>5</b>
<b>3 The Splicer: A Description</b>	<b>8</b>
<b>4 The Splicer: Operation and Maintenance</b>	<b>13</b>
<b>5 Linear Scanners: Methods of Data Collection</b>	<b>18</b>
<b>6 The Splicer: Research and Results</b>	<b>32</b>
<b>7 XY Scanners: Photomultiplier Response Uniformity</b>	<b>38</b>
<b>LIST OF REFERENCES</b>	<b>45</b>

# List of Tables

6.1	Tensile Strength: Kuraray versus Bicon. A long heating time and high pressure make stronger splices. The apparent greater strength of the Bicon fiber is due to the mismatch in sizes for the Kuraray fiber (no clear Kuraray of the proper size was available during this test). .	36
6.2	Comparison of Kuraray Y11(250) Non-S and S type fibers. The only property in which the S type fiber excels is in bending radius. For our application, this was secondary to light transmission and Non-S type was chosen. . . . .	36
6.3	Fiber End Preparation: Razor Blade versus Diamond Polisher. The Diamond Polisher significantly improves the splice quality and adds only 2 minutes of preparation time per splice. . . . .	37
6.4	Study of a large batch of spliced fibers. After a 40 fiber learning curve, the quality of the splice improves. While the bad splices seem worse than the good, some of the worst splices are in the good group. . . .	37



# List of Figures

1.1	Overview of the planned CDF Endplug Upgrade. The light from the tile is routed through Y11(250) 0.83 mm $\phi$ fiber spliced to 0.83 mm $\phi$ clear fiber connected to 0.9 mm $\phi$ clear fiber. The 0.9 mm $\phi$ fiber leads to the decoder box where the light is summed by tower. . . . .	3
2.1	The original coil splicer, used to construct a spaghetti calorimeter. The user placed the ends of the fiber to be spliced in the glass tube, applied pressure with his fingers and depressed the foot pedal to start the cycle.	6
3.1	Overview of the semi-automatic splicer. During the splicing cycle the glare shield is lowered to protect the eyes of the user. . . . .	9
3.2	Closeup of the splicer: view of the halftubes, clamps and lamp. . . . .	10
4.1	Timing diagram for the semi-automatic splicer. . . . .	14
5.1	Data from manual scans of spliced fibers. By plotting on a semi-log scale, the data is linear and the splice easier to see. The bump is due to light being trapped in the sleeve. . . . .	20
5.2	Data from manual scans of a spliced fiber. The upper plot is the raw data: the solid line is the unspliced fiber and the dashed line the fiber after splicing. The lower plot is unspliced/spliced and is easier to interpret. It also makes visible any change in attenuation length due to a poor splice. . . . .	21
5.3	Scan of fiber using linear scanner. The top figure is a plot of the normalized data: the data for the fiber with splice is divided by the data for the fiber without the splice. Two lines are fit to the data— one between the splice and the PMT, and one beyond the splice to the end of the fiber. By dividing the fit to the data beyond the splice by the fit to the data before the splice, the transmission is obtained. This is shown in the bottom plot. A poor splice was intentionally selected to emphasize the location of the splice. . . . .	22
5.4	Photodiode box for use with the multiple fiber linear scanner. The fiber is inserted in the nylon bolt until it reaches the photodiode. The bolt is then firmly screwed on. This applies pressure to the rubber washer and holds the fiber well but does not damage the cladding. . .	24

5.5	Fit of the function $par(1)\exp(-x/par(2))+par(3)\exp(-x/par(4))$ to the data for the unmirrored fiber. $par(2)$ is the short attenuation length of the fiber; $par(4)$ is the long attenuation length. . . . .	26
5.6	Fit of the function $par(1)(75-x) + par(2)$ to calculated values for $R_m$ . This functional form is then used in the program to determine $R_m$ at the desired position. . . . .	28
5.7	Comparison of expected light output and measured light output. The agreement is quite good for the entire length of the fiber. . . . .	29
5.8	Plot of pigtail data taken with multiple fiber linear scanner. The first dip is due to a piece of tape holding the calibration fibers; the second is due to the connector. . . . .	30
6.1	Comparison of good, reasonable and bad splices. The bad splices are indeed lower than average, but some of the good splices are equally poor. Many of the fibers were not measured before splicing and used a standard fiber for normalization. This results in a few splices with apparent transmission over 100%. . . . .	35
7.1	Detail of the $x-y$ scanner. Light from the LED passes through the 1 mm $\phi$ clear fiber to the calibration tube and to scanning point. The scanner has 1 mm resolution. . . . .	39
7.2	The collimator is used when determining the uniformity. However, when studying light mixers, it must be removed. Light from a real fiber will not be collimated and collimated light cannot be mixed. . .	41
7.3	The upper plot is a scan of a bare photomultiplier using the collimator. The lower plot is a scan of the same photomultiplier with a 40 mm light mixer, the collimator, and a 5 mm $\phi$ black dot placed in one corner. Each line on the contour plot is 5%. . . . .	43
7.4	Both plots are with a 40 mm light mixer but without the collimator. The upper plot is with the dot; the lower is without it. The light mixer effectively mixes the light and removes the effect of the dot, with a 4% reduction in output. Each line on the contour plot is 5%. . . . .	44

# Chapter 1

## Introduction

The ability to investigate certain physics topics using the Colliding Detector Facility (CDF) detector at Fermi National Accelerator (FNAL) is limited by the speed and resolution of the current endplugs. When the Main Injector Upgrade is completed, providing more proton and anti-proton bunches and a smaller crossing time, the performance of the gas calorimetry used in the current endplugs will degrade significantly. To provide faster, better endplugs, an upgrade to a (lead + iron)/scintillating sampling calorimeter has been designed and is being constructed. The performance criteria require a calorimeter whose resolution should be approximately  $80-90\%/\sqrt{E} \oplus 5\%$ . This requirement has implication on the light yield since photostatistics must be folded into the intrinsic resolution due to sampling. Also, the 5% constant term requires that variation of the tile-to-tile light yield be better than about 10% and the transverse uniformity be better than 5%. Second, the calorimeter should be able to clearly identify muons. Finally, the segmentation should allow physics topics, such as b-physics, W, Z, and  $\gamma$  physics and jet physics, to be done in an efficient and productive fashion. The criteria must be weighed against cost, radiation hardness properties and ease of construction.<sup>1</sup>

In the new plugs, the scintillating tiles are made of Kuraray SCSN38. Optical

---

<sup>1</sup>See Reference [1]

fibers are used to transmit the light from the tiles to the photomultiplier tubes. The light in the tile is collected by 0.83 mm $\phi$  Kuraray Y11(250) green wavelength shifting (WLS) fibers which lie in grooves machined in the scintillator, and passes through 0.83 mm $\phi$  clear fibers to the edge of the megatile. From there, 0.9 mm $\phi$  clear fibers transmit the light to the decoder box, where 1.0 mm $\phi$  fibers are used to sum the signals by tower (Figure 1.1). Michigan State University is responsible for producing all of the necessary fiber optics for the hadron calorimeter, from the fibers in the tiles to the photomultiplier tube decoder boxes. The 0.83 mm $\phi$ -to-0.9 mm $\phi$  and 0.9 mm $\phi$ -to-1.0 mm $\phi$  joints are accomplished using injection molded flat connectors. The fibers are glued into these connectors in groups of 8 or 9 (known as a pigtail) and the face is polished using a diamond polisher. The conversion from WLS fiber to clear fiber is more complex.<sup>2</sup>

Since a given fiber is extruded from a single boule, it is impossible to manufacture a single fiber that simply stops wavelength shifting at some point. As the fibers are made of a plastic with a reasonable melting point, it is easy to imagine heating the ends of two fibers while pushing them together, and allowing them to cool. This would produce a single fiber that is wavelength shifting for part of its length and still has an overall attenuation length that is long enough to allow the fiber to deliver sufficient light to a photomultiplier tube.

The construction of the detector will include two plugs and a test beam module. Each plug has 22 hadron layers, each layer 12 megatiles, each megatile four pigtails and each pigtail 9 fibers. This totals approximately 20,000 splices for the hadron calorimeter. For this operation to be successful, an dependably repeatable, easy to use device had to be constructed. The Michigan State University semi-automatic

---

<sup>2</sup>The transition from WLS fiber to clear fiber is necessary as the doping agents in WLS fiber result in a short attenuation length—2.2 meters. The attenuation length of clear fiber is 8.6 meters.

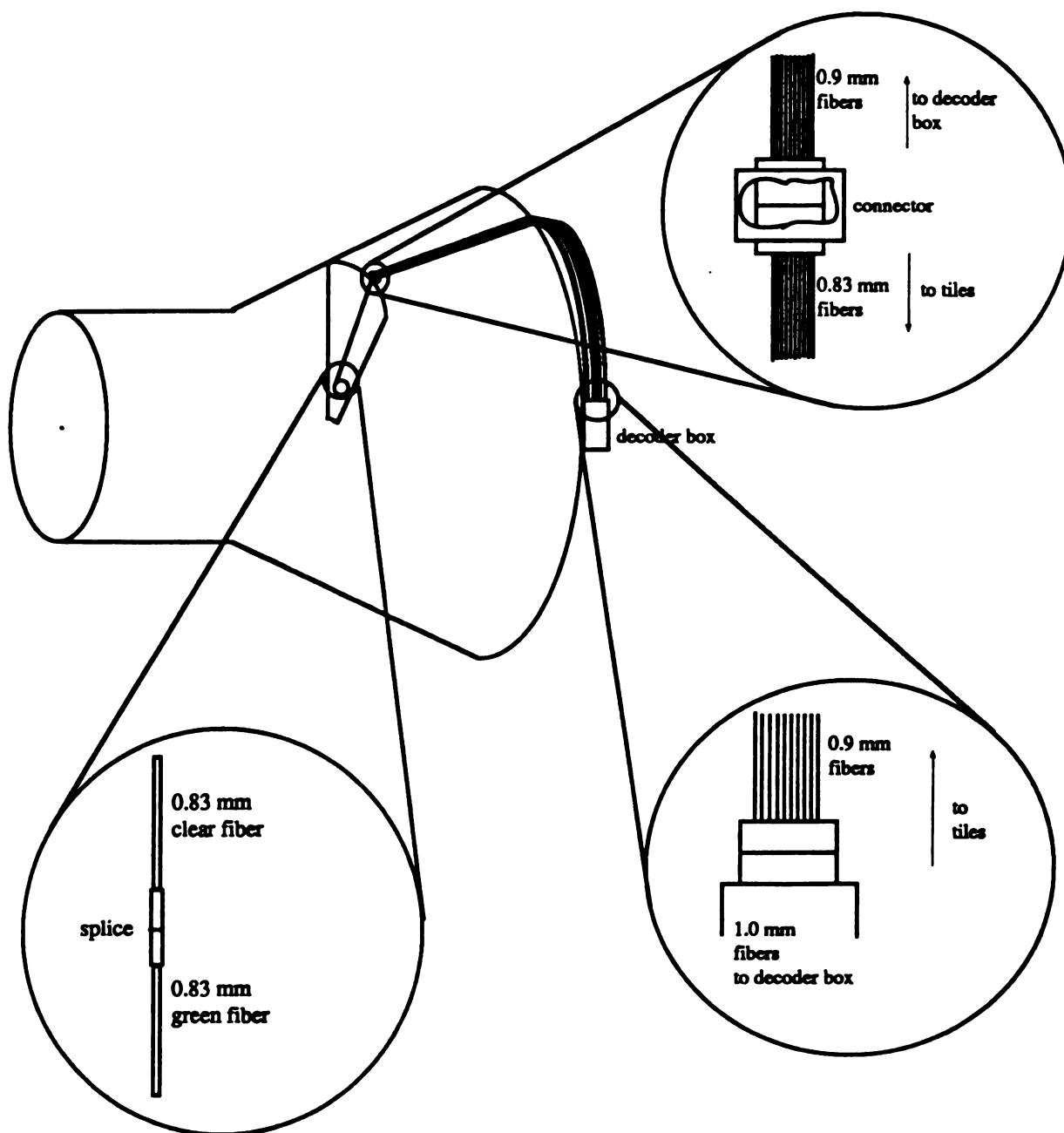


Figure 1.1: Overview of the planned CDF Endplug Upgrade. The light from the tile is routed through Y11(250) 0.83 mm $\phi$  fiber spliced to 0.83 mm $\phi$  clear fiber connected to 0.9 mm $\phi$  clear fiber. The 0.9 mm $\phi$  fiber leads to the decoder box where the light is summed by tower.

splicer is such a device and it is presently being used in the endplug assembly.

# Chapter 2

## History

The first splicer built at Michigan State University bears little semblance to the final product. Based on a machine designed at Fermilab<sup>1</sup>, it consisted of a simple coil of nichrome connected to a transformer (Figure 2.1) and was used to build a spaghetti calorimeter for T-840. The user placed the ends of the fibers to be welded in a glass tube and pressed them together while the coil heated and melted them. The first refinement replaced the fingers with a spring loaded clamp to provide somewhat more consistent pressure on the fibers. This device did produce spliced fibers: the quality of the splice was acceptable but the physical strength of the weld was very poor.<sup>2</sup>

In an SSC/GEM related effort, a split welding tube machine was designed to consistently hold and push the fiber while providing uniform heating. A clamp firmly holds the fiber and gently applies pressure to maintain contact between the fiber ends being spliced. A treated slide projector bulb is used to provide uniform, controllable heat at the splice joint (see below for a complete description of the splicer). Refinements to this machine include a cooling cycle, adjustable heating time and horizontal pressure, and myriad safety features.

---

<sup>1</sup>See Reference [2]

<sup>2</sup>See Reference [3]

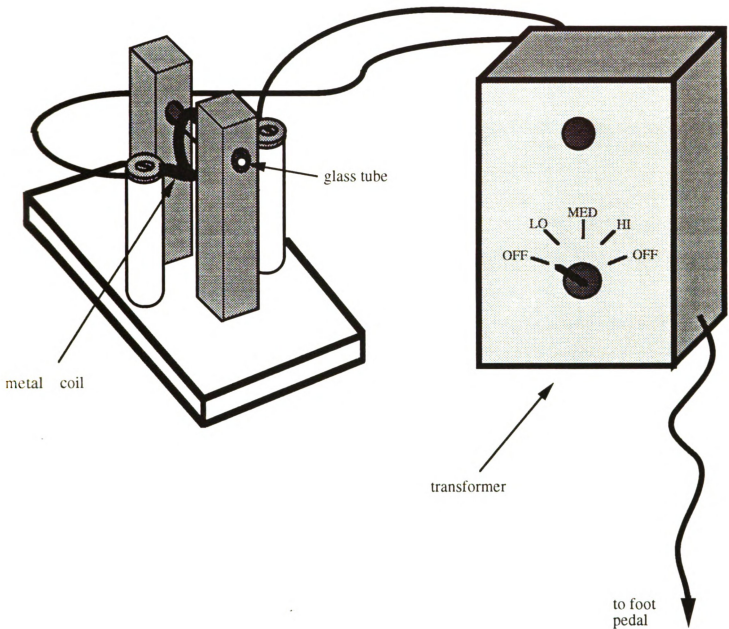


Figure 2.1: The original coil splicer, used to construct a spaghetti calorimeter. The user placed the ends of the fiber to be spliced in the glass tube, applied pressure with his fingers and depressed the foot pedal to start the cycle.



At present, seven final splicing machines exist— four at Fermilab, two at Michigan State and one in Japan at the University of Tsukuba. Michigan State is in the process of building more to be sent to various laboratories around the country.

## Chapter 3

# The Splicer: A Description

The splicer is a deceptively simple looking device (Figure 3.1). The heart of the machine is two half-round glass tubes (Figure 3.2). These tubes, plus the use of an FEP sleeve around the splice joint, are what make the Michigan State splicer unique. The bottom tube is anchored and the top tube has one inch of vertical motion. In the open position, the fiber can easily be inserted and removed. In the closed position, the half tubes meet to form a whole tube whose inner diameter is exactly the outer diameter of the fiber plus FEP sleeve. This holds the fiber during the splicing operation without allowing the joint to buckle or swell. Since the half tube is quite fragile and susceptible to breaking, a whole tube is positioned underneath to add support. The ends of the whole and half tubes are in a U-shaped piece of steel, collectively referred to as a cassette. Two cassettes are in a set (top and bottom) and are perfectly matched— if one is broken, the entire set must be replaced. On either side of the cassettes are a set of rubber clamps. The upper and lower clamps have a 1 mm deep groove milled along the center. In addition, the lower grooves have holes drilled in them. The insides of the lower clamps are hollow and connected to a small pump, which is used to draw a light vacuum to hold the fiber in place prior to closing the clamp. The right clamps are firmly fixed, while the left clamps have 0.25" movement to push the ends of the fiber together.

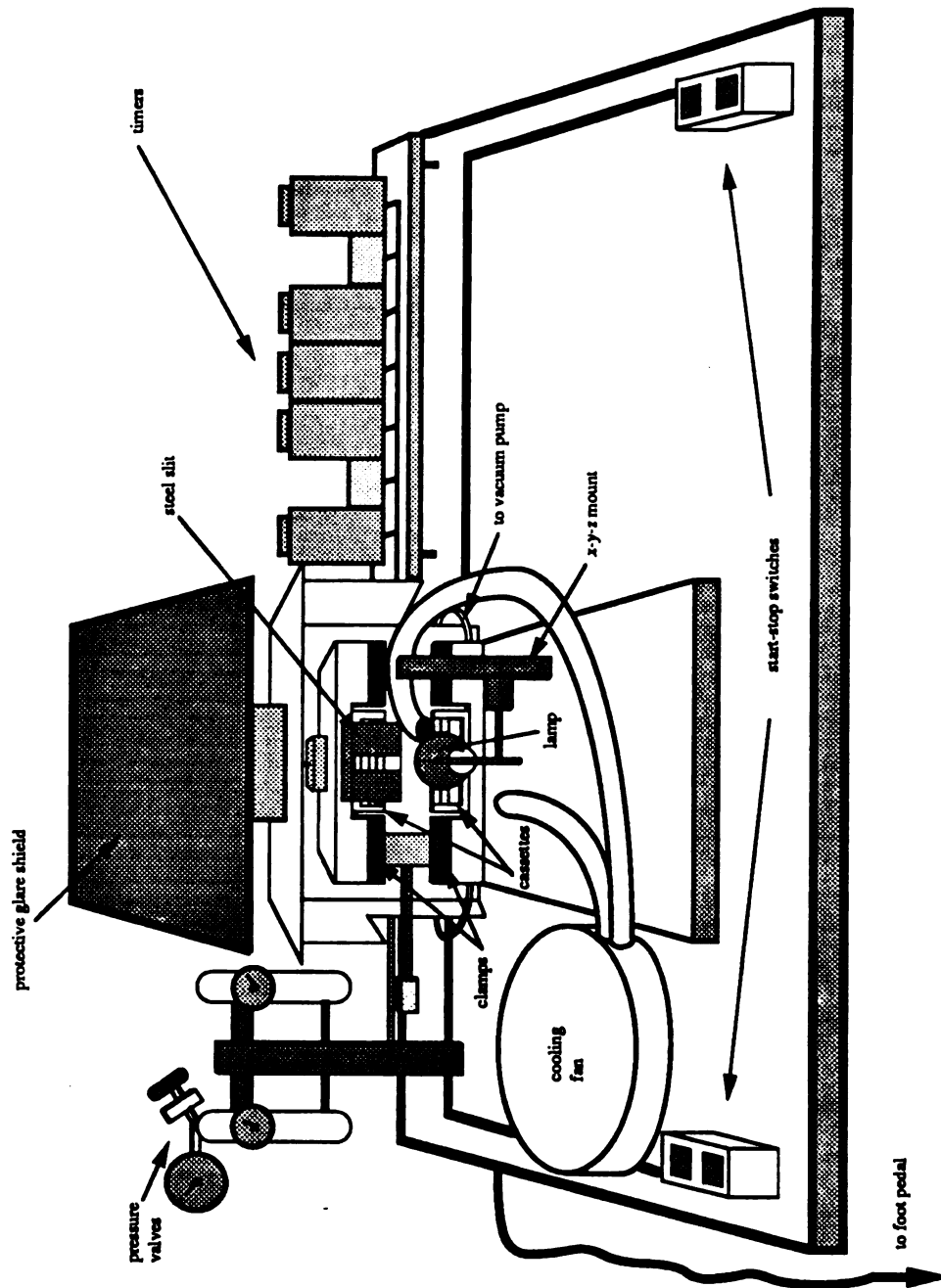


Figure 3.1: Overview of the semi-automatic splicer. During the splicing cycle the glare shield is lowered to protect the eyes of the user.

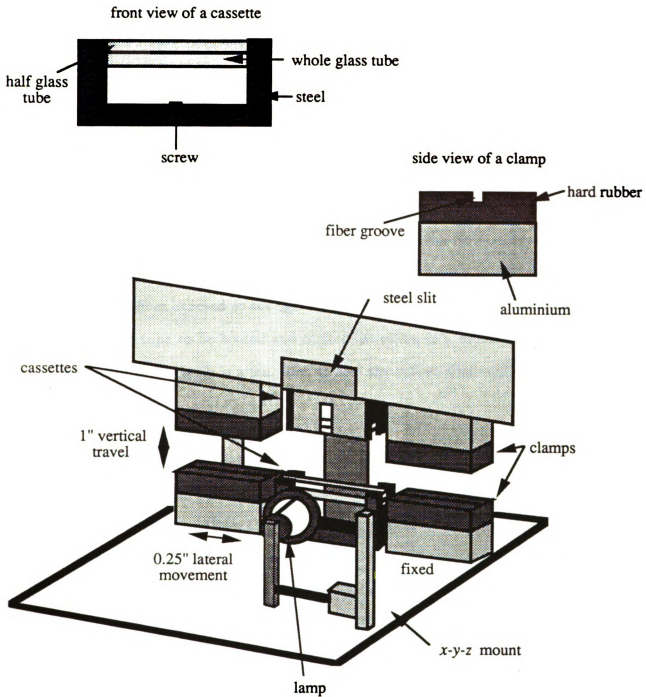


Figure 3.2: Closeup of the splicer: view of the halftubes, clamps and lamp.

Directly in front of the center of the cassette is the slide projector lamp. It is a standard bulb, with the inner side of the reflector coated with 500Å of chrome under 1300Å gold. Gold is used because it is very reflective in the near-infrared region; the chrome provides a better surface to which the gold adheres. The reflector is coated since the original coating is a special dichromatic film that reflects visible light and passes infrared light (enabling one to view one's slides without melting them). The lamp is positioned roughly 2" from the cassette placing the focal point directly on the middle of the cassette. The lamp is attached to a *x-y-z* mount that allows the lamp to be easily adjusted in all three directions. Between the lamp and cassette, attached to the upper clamp, is an 0.008" thick steel shim, bent and slotted to reduce the amount of fiber exposed to the light. The slit allows only a small fraction of the fiber in the half tube to be heated and melted, resulting in a better splice. In front and to the left of the lamp is a fan, used to cool the spliced fiber and the lamp assembly after heating.

The remainder of the splicer is timers, switches and valves. In the front corners are the start and stop switches. As a safety feature, both start switches must be pressed at the same time; the stop buttons function independently. In the left rear are the pressure regulators, connected to house air. The right one controls the vertical pressure; it is generally set to 100 psi. The front left regulator is used to reduce the pressure reaching the rear regulator, which controls the horizontal pressure. A 10:1 converter is used to reduce the pressure to the needed level and the horizontal pressure can be adjusted in 0.05 psi increments from 0 psi to 3.0 psi. In the right rear corner of the splicer are the 5 timers. They have adjustable ranges, from 0-6 seconds, 0-60 seconds and 0-6 minutes. They allow complete control of the various cycles of the splicer, easily changed to accommodate the times needed for various types of fibers. The timers used in the U.S. version are 60 Hz; the Japanese splicer uses 50 Hz in

accordance with local electrical supply.

There are a few additional parts needed for the splicer. A single box contains the switches for main power and a separate control switch for the heater lamp, as well as the 110V to 22V transformer to supply the lamp. The cable from this box to the splicer provides the 22V for the slide projector bulb and the 110V to power the timers, pressure valves and an overhead lamp. In the floor is a small vacuum pump controlled by a foot switch. This pump provides the vacuum for the fiber chuck.

These three components– the pump, the transformer box and the splicer itself– form the package as produced by Michigan State University. The only other necessary supplies are 110 VAC and house air (100 psi minimum). The splicer can be uncrated, set up and used easily and quickly.

# Chapter 4

## The Splicer: Operation and Maintenance

For a general user, the splicer is quite simple to operate. The prepared ends<sup>1</sup> of the fibers to be fused are placed in an FEP sleeve and centered in the bottom half tube and the foot pedal is depressed. The fiber is held in place by the light vacuum from the floor pump. Next, both start buttons are simultaneously pressed and the glare shield is lowered (to reduce the risk to the user and other people in the room). The upper clamp lowers to secure the fibers and timer 1 starts. After timer 1 stops, the horizontal pressure is applied and timer 2 starts. These steps are done separately to ensure grasp of the fiber is complete before attempting to apply horizontal pressure. After timer 2 stops, the heater bulb comes on for the time set by timer 3. When the heating is done, the fan cools the light and the fiber/cassette assembly for the time set by timer 4. When cooling is complete, the horizontal pressure is removed. Finally, after time set by timer 5, the vertical pressure is removed and the clamp opens. Again, these operations are separate tasks to prevent any possible damage to the spliced fiber. As soon as the clamp opens, the fiber can be removed. The timers automatically reset themselves and the splicer is ready to begin again. Figure 4.1 is the timing diagram for all five timers.

---

<sup>1</sup>The ends are prepared using a diamond polisher; see below for details.

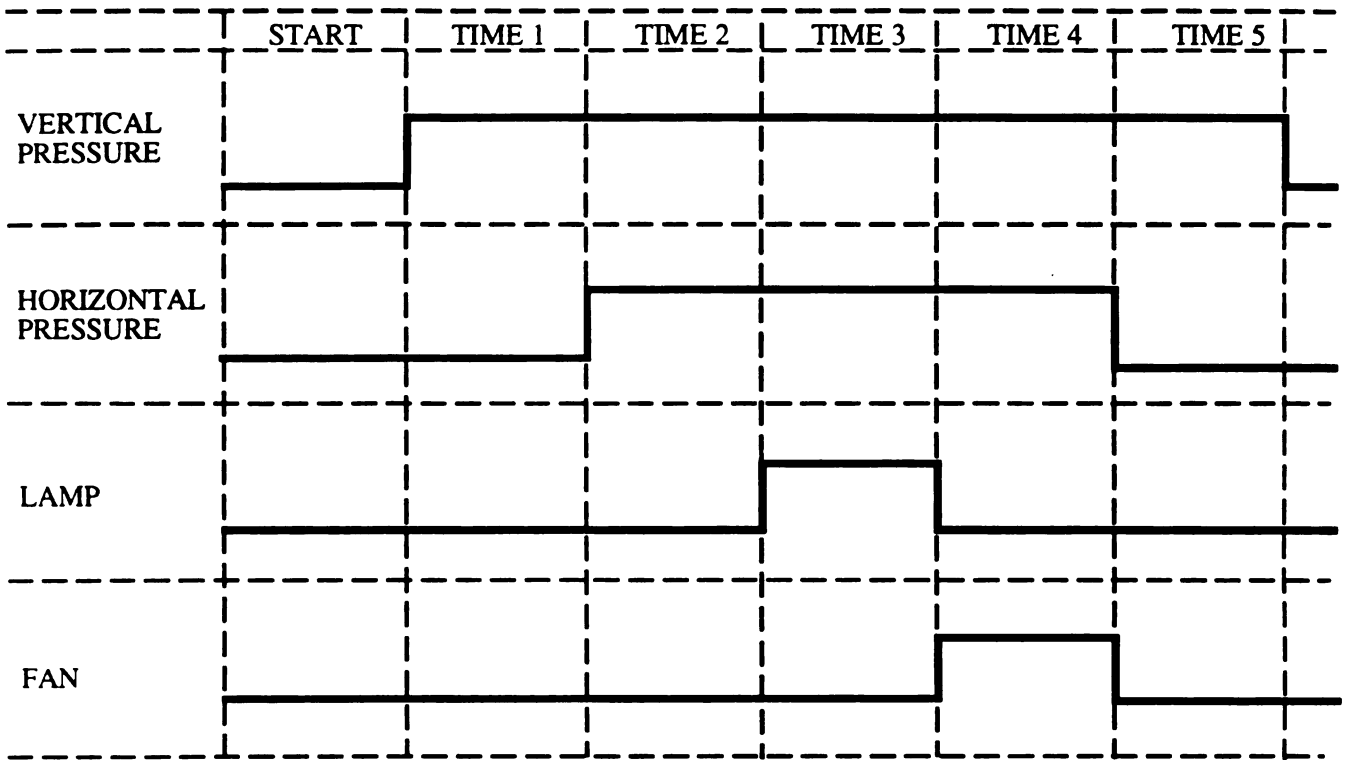


Figure 4.1: Timing diagram for the semi-automatic splicer.



Daily maintenance is necessary to keep the splicer operating at peak efficiency. Every time a fiber is handled, some skin oil is left on the fiber. When the fiber is placed in the half tubes, some of this oil is transferred to the glass and is baked on. Burnt skin oil is dark and opaque and will cause uneven heating of the fiber. This results in uneven melting and poor splice quality. To remove these deposits, the cassettes must be removed. First, the steel slit is removed and the retaining screws in the cassettes are unscrewed. Next, the cassettes are gently pulled from the alignment posts. If this is difficult, it is possible to gently pry them loose with a razor blade. The deposits are now gently scraped off, using a 0.046" gauge pin— this pin should have a slightly smaller diameter than the inner diameter of the half tubes. At this time all four glass tubes should be visibly inspected for wear and damage. If no damage is found, the cassettes are replaced. Since the cleaning and replacement process requires handling of the cassettes, they must be cleaned again. Now a cotton applicator with flux remover is used – this removes un-heated skin oil quite nicely and does not damage the cassette in any way. Finally, the steel slit is replaced. The splicer is now ready for use.

After many splices, the steel slit will become carbonized and the slit itself will widen. This, too, causes a degradation in splice quality. Another slit must be fashioned from 0.008" steel. When returning the slit to the splicer, care must be taken to ensure proper placement. The slit must be centered on the cassette, and it must be placed with the bend towards the cassette.

In general, the maintenance of the splicer is as easy as the operation. However, from time to time serious problems arise, although none will result in permanent damage. The most common serious problem is a broken cassette. This is usually caused by user error— if the fiber is not exactly centered in the half tubes, it will be pinched and crack or chip the half tube. It can also simply wear out— although it

rarely lasts that long. Cassettes are easily replaced, but as this takes a minimum of four hours, it is recommended to have at least two cassettes for each splicer. To replace the cassette, they are first removed from the splicer. The broken tubes are removed. With care, the whole tubes, if not damaged, can be salvaged. However, the half tubes must be removed. If they are unbroken, they can be remeasured and reused later. It is not necessary to remove the whole tubes, but as much RTV is scraped out as possible.<sup>2</sup> If building a new cassette, or if the whole tubes are replaced, the retaining screws are inserted first. Next, some RTV is applied on the cassette and the ends of the whole tubes. A small jewellers screwdrivers works well for applying RTV. Some more RTV is put on the top of the whole tubes and the half tubes are placed the proper position. [See below for instructions of how to choose half and whole tubes and cassettes.] A cotton applicator is used to remove any excess RTV and the cassettes are returned to the machine. This is easier if the bottom cassette is inserted first. A 0.047" gauge pin (or the appropriate size for the half tubes used) is placed in the lower half tube and a wire jumper in the appropriate holes for timer 1. The vertical and horizontal pressures are turned off. The splicer, but not the lamp, is turned on and the upper jaw is manually lowered. The horizontal pressure is slowly increased to 80 psi. The cassettes are inspected for cracks in the glass and left to cure for at least four hours. When curing is complete, the horizontal pressure is slowly reduced, the upper jaw lifted, and the cassette removed. Using a razor blade, any excess RTV is scraped off. The cassette can now be returned to the splicer, timer 1 replaced, and the horizontal and vertical pressures returned to normal. The splicer is ready for use.

When building a cassette, careful selection of all components is important. Since

---

<sup>2</sup>RTV is used as it has a 20-minute working time, cures reasonably rapidly, has reasonable flexibility during curing, can be heated and cooled repeatedly with no loss of strength, and can easily be removed with a razor blade.

each cassette can be used only in the machine in which it was built, each cassette must be labeled. Information on the cassette should include both the machine in which it belongs and whether it is for the top or bottom jaw. When the cassette is in use, 100 psi are exerted on the bottom jaw. The glass half tubes will quickly break if they protrude above the edges of the metal cassette. The level of the half tubes is controlled by the outer diameter of the whole tube— 0.088". The inner diameter of the half tubes is constant; the outer diameter can vary by as much as 0.002". This slop can be removed by pairing an oversized half tube with an undersized one. Properly sized parts make a cassette that will generally last until user error damages it.

The only other easily replaced item is the slide projector bulb. Our bulbs have 500Å chrome under 1300Å gold. Careful degreasing and an overnight session in an evaporator will properly prepare the bulbs. After a bulb is in place, it must be positioned so the hottest spot is centered on the middle of the cassette. Silphos<sup>3</sup> will ignite quickly at the temperature provided by the bulb and thus provides an easy locator for the focal point. Stopping the light cycle as soon as the metal burns and moving the bulb in all three dimensions using the *x-y-z* mount will allow the bulb to be properly positioned. The *x*- and *y*-axes are easily done; the *z*-axis is harder to do but equally important. It can take some time to align the bulb but practice makes this easier.

---

<sup>3</sup>Silver phosphorous copper brazing alloy, used in refrigeration.

## Chapter 5

# Linear Scanners: Methods of Data Collection

When building a device as complex as the plug hadron calorimeter upgrade, it is necessary to have methods of testing and quality control at every step of the assembly. The splices and pigtails must be tested to ensure consistent quality. There are two possible methods to stimulate the spliced fiber and thus measure the light output. One is to place the end of the fiber in a scintillating tile and place a radioactive source near the tile. The other is to shine an ultraviolet light directly on the fiber. The second method is preferable, as it is safer, and can be used to provide measurements of position versus light output.

Our early measurements were accomplished with a simple device. A UV light bulb was wrapped in vinyl electrical tape, leaving only a small hole exposed. A 1 mm inner diameter glass tube was positioned over the hole, tangent to the bulb, and the fiber to be tested was drawn through the tube. The end of the fiber was placed in contact with a photomultiplier tube. By moving the UV bulb along the length of the fiber, position versus light output measurements were made. The data were entered into a computer and a graph plotted using a semi-log scale. By comparing the value directly before the splice to the value directly after, a rough calculation of

the transmission was calculated (Figure 5.1).

In the next iteration of tests, the light output for an uncut fiber was measured as a function of position. The fiber was then cut, spliced and re-measured. As can be seen in Figure 5.2, this made the data much easier to interpret and removed such systematic errors as fiber placement near the photomultiplier and small variations in the position of the UV bulb. However, this method of data collection was very time consuming and subject to positional errors.

To improve the quality of the data collected and reduce the time necessary to scan a fiber, an automated linear scanner was built. A six-foot long section of 1" PVC pipe with a groove milled along the length serves as a vacuum chuck for the fiber to be tested. A UV light source attached to a cart moves along the length of the fiber. The motion of the cart is accomplished by a threaded rod which runs beneath the pipe and passes through a stepper motor which is attached to the cart. By spinning a nut inside the motor, the cart can be made to move along the rod. The entire device is controlled and read out using CAMAC. The position of the light was easily controlled to less than 0.25 mm. A program was written so the data is plotted on a terminal as it is collected.

For this device, a clear fiber is spliced to a green fiber. The free end of the clear fiber is placed near the face of a photomultiplier and the program is run. The fiber was removed, the green fiber cut and spliced and the fiber then rescanned.<sup>1</sup> The two scans are compared and the transmission across the splice calculated. A typical scan takes 20 minutes. A sample fiber scan is shown in Figure 5.3.

For the construction of the plug upgrade, it is impractical to scan each individual fiber, especially since this would take over 1000 days. Instead, a pigtail scanner was

---

<sup>1</sup>Merely scanning the green-clear splice will not provide any useful information. The clear fiber does not respond to the UV lamp and 0 is read until the light is over the green fiber.

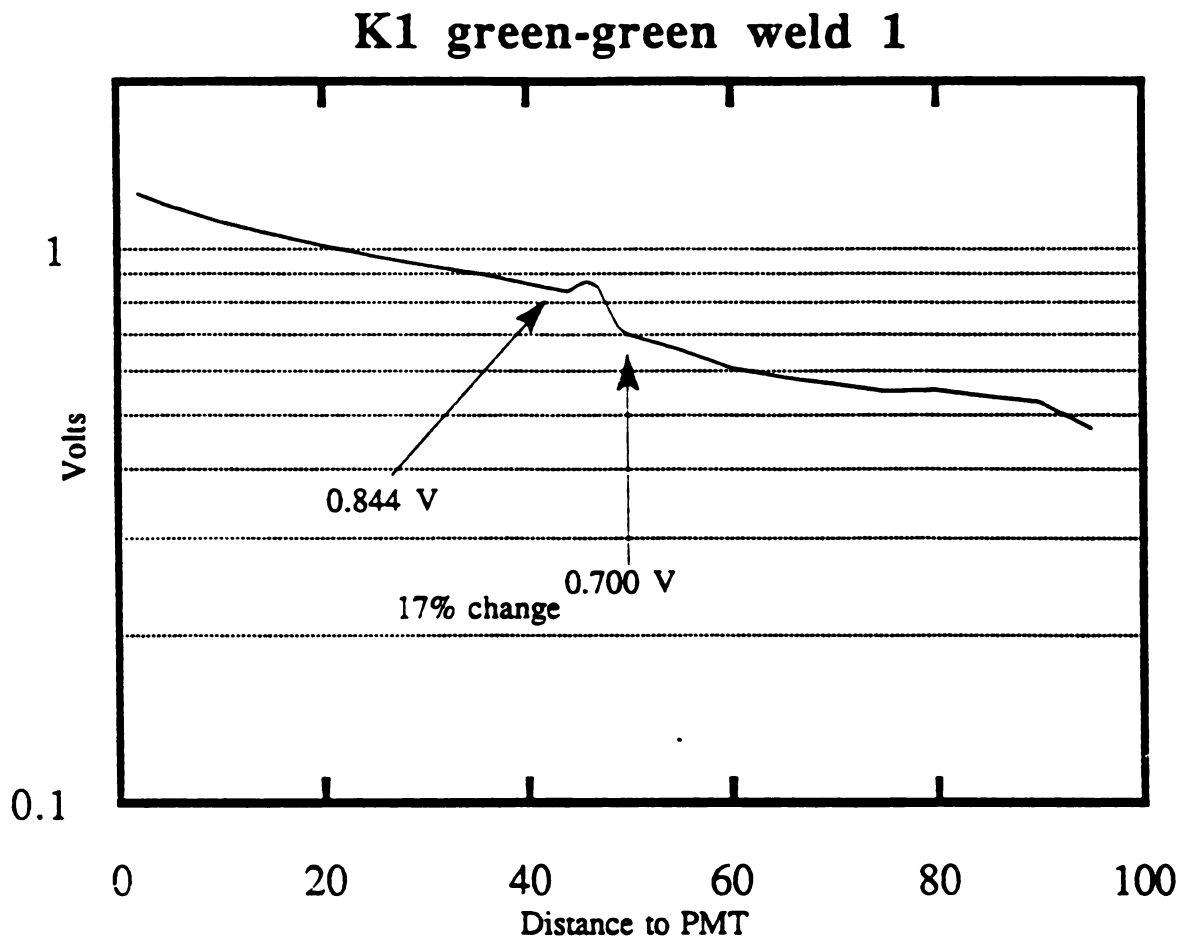


Figure 5.1: Data from manual scans of spliced fibers. By plotting on a semi-log scale, the data is linear and the splice easier to see. The bump is due to light being trapped in the sleeve.

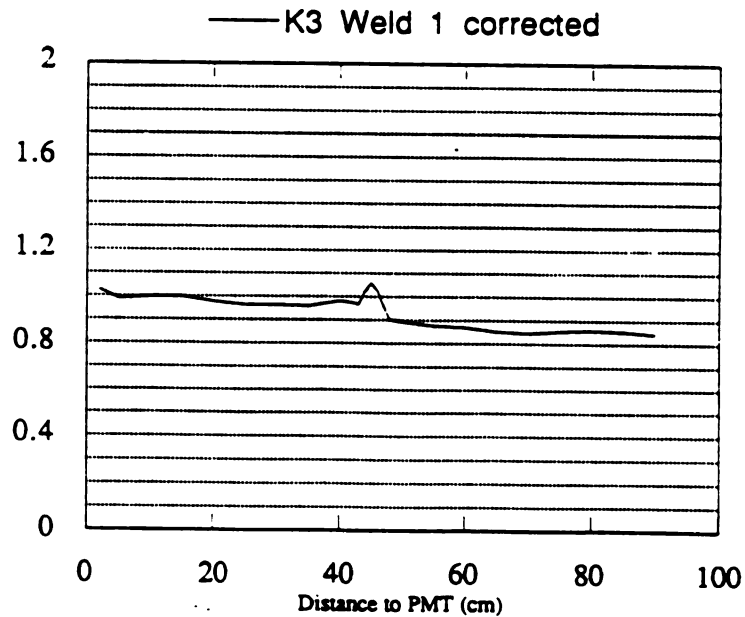
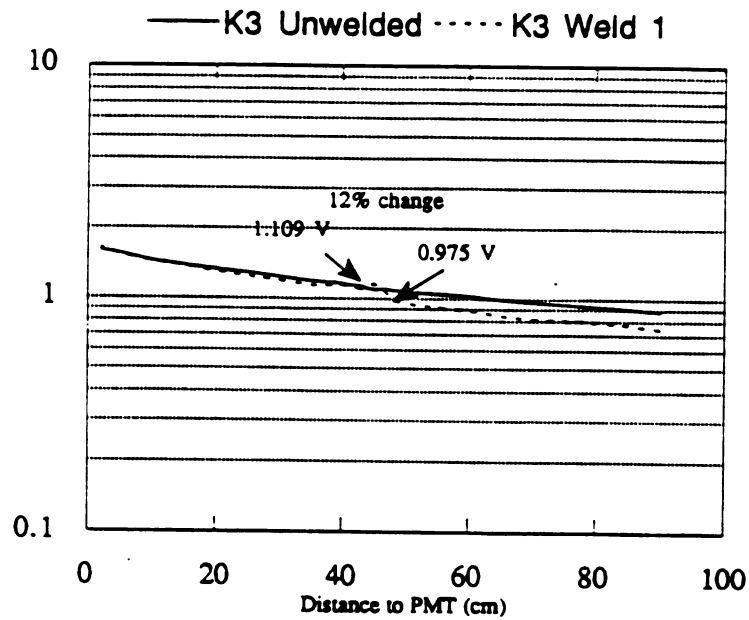


Figure 5.2: Data from manual scans of a spliced fiber. The upper plot is the raw data: the solid line is the unspliced fiber and the dashed line the fiber after splicing. The lower plot is unspliced/spliced and is easier to interpret. It also makes visible any change in attenuation length due to a poor splice.

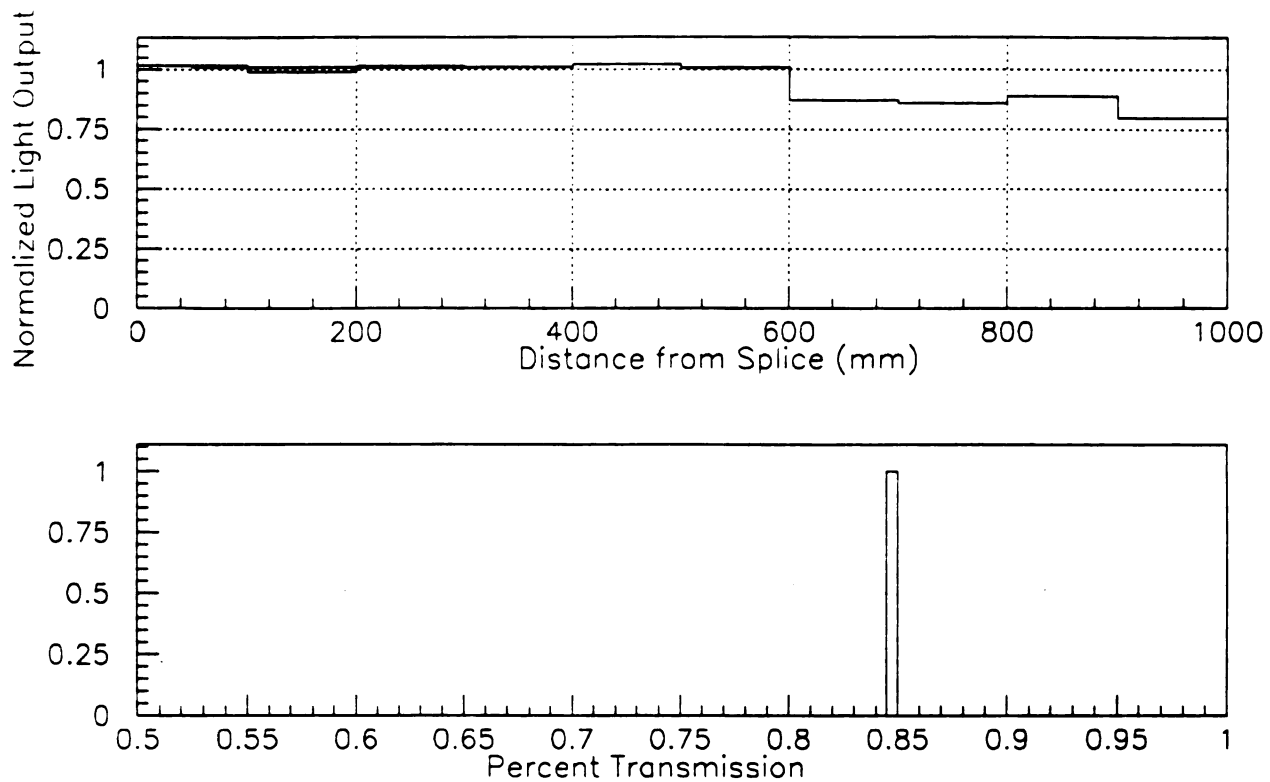


Figure 5.3: Scan of fiber using linear scanner. The top figure is a plot of the normalized data: the data for the fiber with splice is divided by the data for the fiber without the splice. Two lines are fit to the data— one between the splice and the PMT, and one beyond the splice to the end of the fiber. By dividing the fit to the data beyond the splice by the fit to the data before the splice, the transmission is obtained. This is shown in the bottom plot. A poor splice was intentionally selected to emphasize the location of the splice.



built. This device is capable of scanning an entire pigtail (8-9 fibers) in 20 minutes, keeping pace with the assembly of the pigtails. It is necessary to have the ability to determine the percent transmission of each green to clear splice. Using a similar design to the single fiber scanner, a pigtail scanner was constructed to make these measurements possible. A 2" by 8' piece of PVC with 10 grooves milled along the length and holes drilled at regular intervals is glued to a chamber that is attached to a large vacuum pump. This serves as a fiber chuck to hold the pigtail stationary during the scan. A 3" UV pen lamp, inside a box with only a 1 mm by 3" slit opening, is attached to a belt driven cart. The cart moves in 1 cm steps along the fibers. For general use, the pigtail is placed in the grooves and the connector snapped into a connector box. The other side of the connector box is occupied by a connector containing 9 green fibers, which lead to a photodiode box (Figure 5.4). Each fiber is connected to a photodiode, which in turn is connected to a switchbox.<sup>2</sup> The switchbox is controlled through CAMAC and feeds a single, switchable output to a picoammeter. The picoammeter is read out through GPIB at 2Hz, the maximum usable rate.<sup>3</sup>

After the data is taken, it must be examined to determine the quality of the splice. Each fiber is normalized by dividing all the data for that fiber by the value at a point close to the connector on the photodiode side. This removes the dependence on the photodiode and any small variation in the light source. Next, the transmission through the splice and connector is calculated, using the formula

$$\text{Transmission} = \frac{\text{normalized light output}(x)}{\exp(-l_1/\lambda_{\text{green}}) \exp(-l_2/\lambda_{\text{clear}})(F(x) + R_m F(2l_3 - x))}$$

where *normalized light output*(*x*) is the measured value at point *x*, *l*<sub>1</sub> is the length of the green fiber between the calibration point and the connector (constant), *λ*<sub>green</sub>

<sup>2</sup>Designed and constructed by Bill Kinney, FNAL.

<sup>3</sup>The scanner was originally designed to take measurements using a LeCroy 2249A ADC through CAMAC. This would have resulted in a device capable of scanning 10 channels of 2+ meters of fiber in less than two minutes. Unfortunately, the photodiodes used do not produce a strong enough signal and must be read out using the picoammeter.

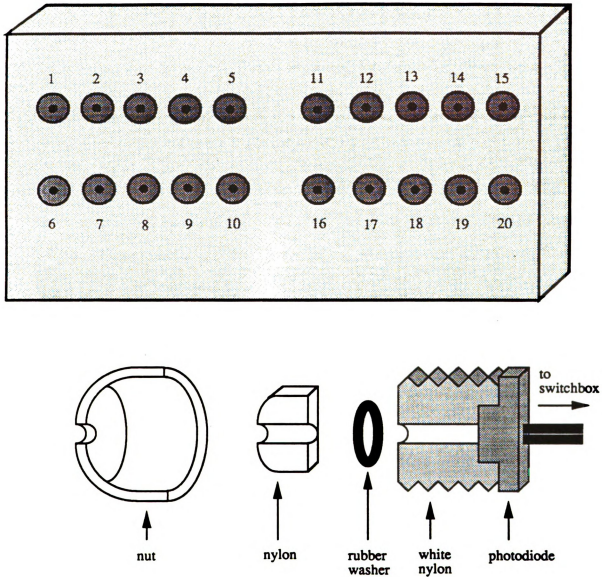


Figure 5.4: Photodiode box for use with the multiple fiber linear scanner. The fiber is inserted in the nylon bolt until it reaches the photodiode. The bolt is then firmly screwed on. This applies pressure to the rubber washer and holds the fiber well but does not damage the cladding.

is the long attenuation length of the green fiber (constant),  $l_2$  is the length of the clear fiber between the connector and the splice (determined by the program),  $\lambda_{clear}$  the attenuation length of the clear fiber (constant), and  $l_3$  is the length of the spliced green fiber (determined by the program). All of these parameters are determined by the program during execution and are generally different for different pigtailed.

$F(x)$  is

$$F(x) = 0.27 \exp(-x/\lambda_1) + 0.73 \exp(-x/\lambda_2)$$

and is the expected light output when the fiber is excited at point  $x$ .  $\lambda_1$  is 12.3 cm, the short attenuation length of the green fiber, and  $\lambda_2$  is 222.2 cm, the long attenuation length. These constants were determined by scanning ten 70 cm long fibers each spliced to a 1 m long clear fiber. The average values for all ten fibers were read into a histogram and the formula

$$par(1) \exp(-x/par(2)) + par(3) \exp(-x/par(4))$$

was fit to the data. The resulting plot is Figure 5.5.

Naively, one would expect  $R_m$ , the effective reflectance of the mirror, to be a constant. However, because of the two different attenuation lengths and imperfections in the mirrored surface, the effective  $R_m$  is a function of  $x$ .  $R_m$  was determined by scanning ten 70 cm mirrored fibers. The mirrored ends of the fibers were then cut off at 45°, the ends were blackened, and the fibers rescanned. The expected light output for an unmirrored fiber is

$$F_1(x) = F(x)$$

and the expected light output for a mirrored fiber is

$$F_2(x) = \underbrace{F(x)}_{\text{transmitted}} + \underbrace{R_m F(2L - x)}_{\text{reflected}}$$

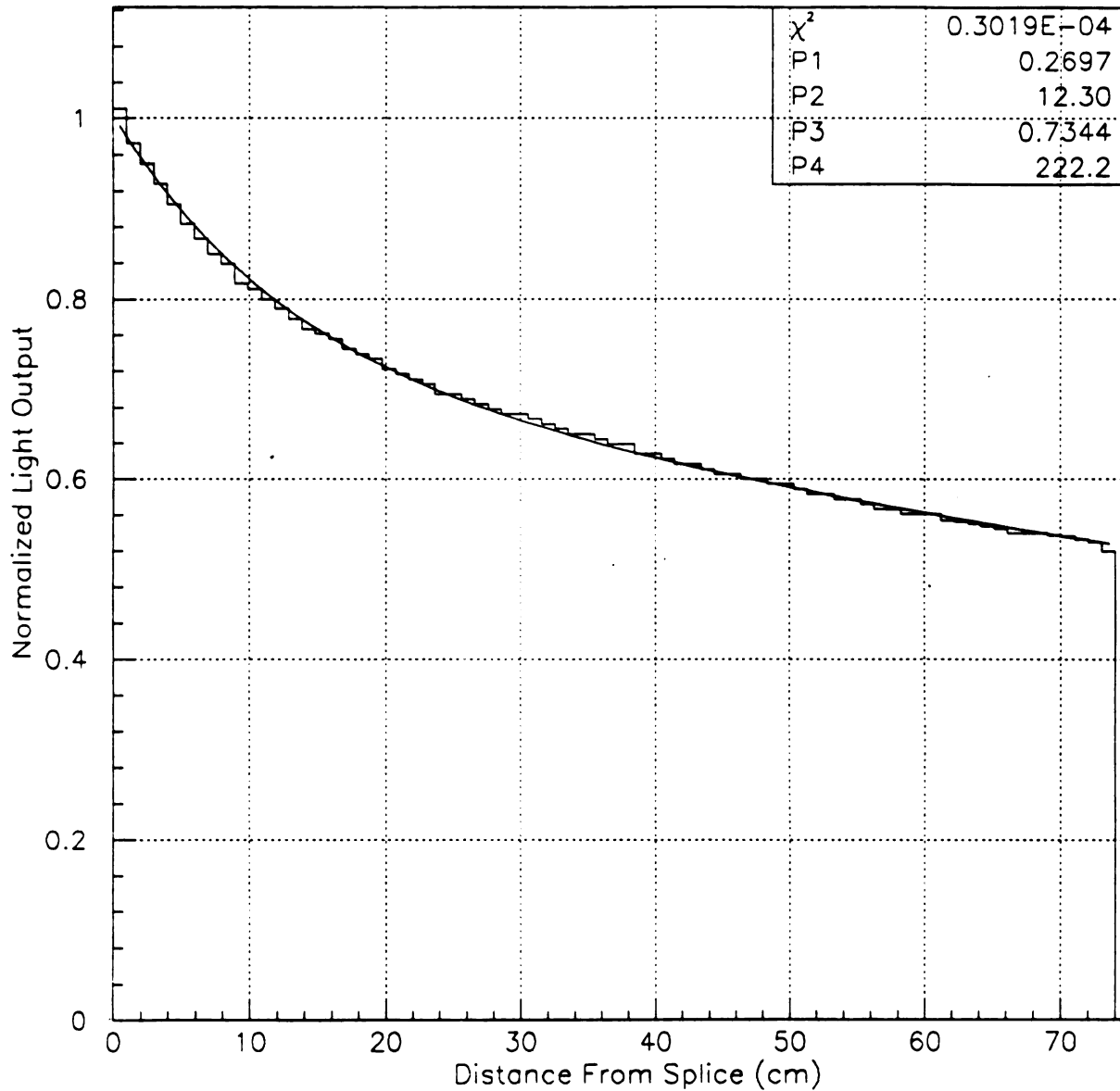


Figure 5.5: Fit of the function  $par(1)\exp(-x/par(2))+par(3)\exp(-x/par(4))$  to the data for the unmirrored fiber.  $par(2)$  is the short attenuation length of the fiber;  $par(4)$  is the long attenuation length.

By solving for  $R_m$ , one gets

$$R_m(x) = \left( \frac{F_2(x)}{F_1(x)} - 1 \right) \frac{F(x)}{F(2L - x)}$$

$F_2(x)$  is the measured light for the mirrored fiber and  $F_1(x)$  is the measured light output for the unmirrored fibers. The values for  $R_m(x)$  were placed in a histogram and the function

$$par(1)(L - x) + par(3)$$

was fit to the data. The results from this fit are in Figure 5.6 and produce the functional form

$$R_m(x) = 0.00163(l_3 - x) + 0.82$$

that is used in the program. This function is valid for  $30 \text{ cm} < l_3 < 100 \text{ cm}$ ; for  $l_3 < 30 \text{ cm}$   $R_m(x)$  simply becomes 0.80, a constant. A comparison between the calculated and measured light output for a mirrored fiber is shown in Figure 5.7.

The transmission through the splice and connector is calculated at three points and averaged. This information, as well as the raw light output 5 cm beyond the splice, is output to a file. The file also contains the normalized data. Plots of the normalized data are shown in Figure 5.8. The information in the plot is saved for future reference.

This linear scanner will perform additional functions needed in the plug upgrade construction. Each batch of Y11(250) fiber must be checked to ensure consistent quality. The attenuation lengths of the Y11(250) fiber can be easily measured using the scanner and then compared with previously measured values. To test the clear fiber, 1 m green fiber is spliced to 2 m of clear fiber. The fiber is scanned and 1 m clear fiber removed. The fiber is re-scanned and the results are compared to determine the attenuation length of the clear fibers. In this way, the mean attenuation length for a sample of 10 fibers can be compared with the standard value. The other main use of

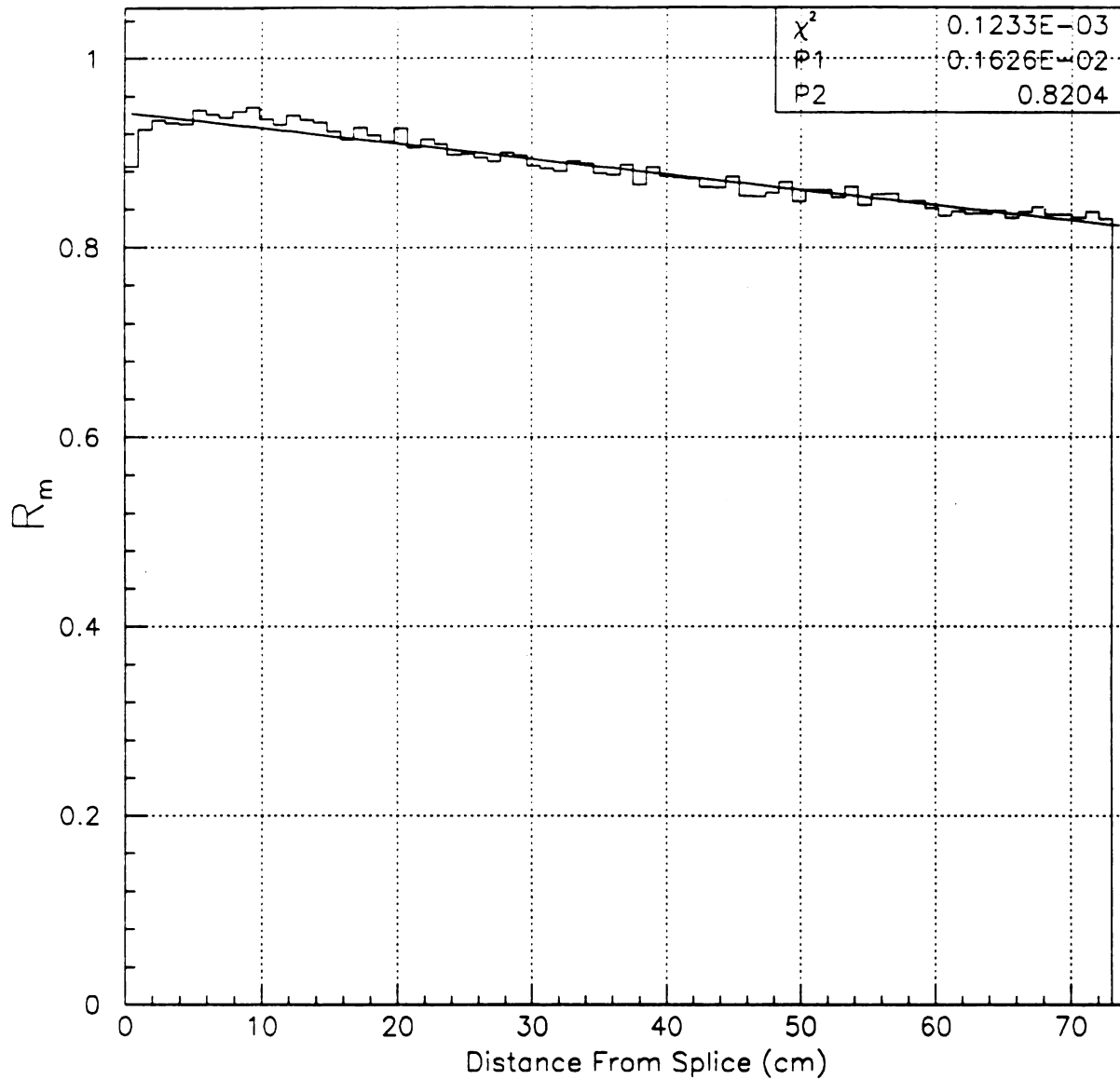


Figure 5.6: Fit of the function  $par(1)(75-x) + par(2)$  to calculated values for  $R_m$ . This functional form is then used in the program to determine  $R_m$  at the desired position.

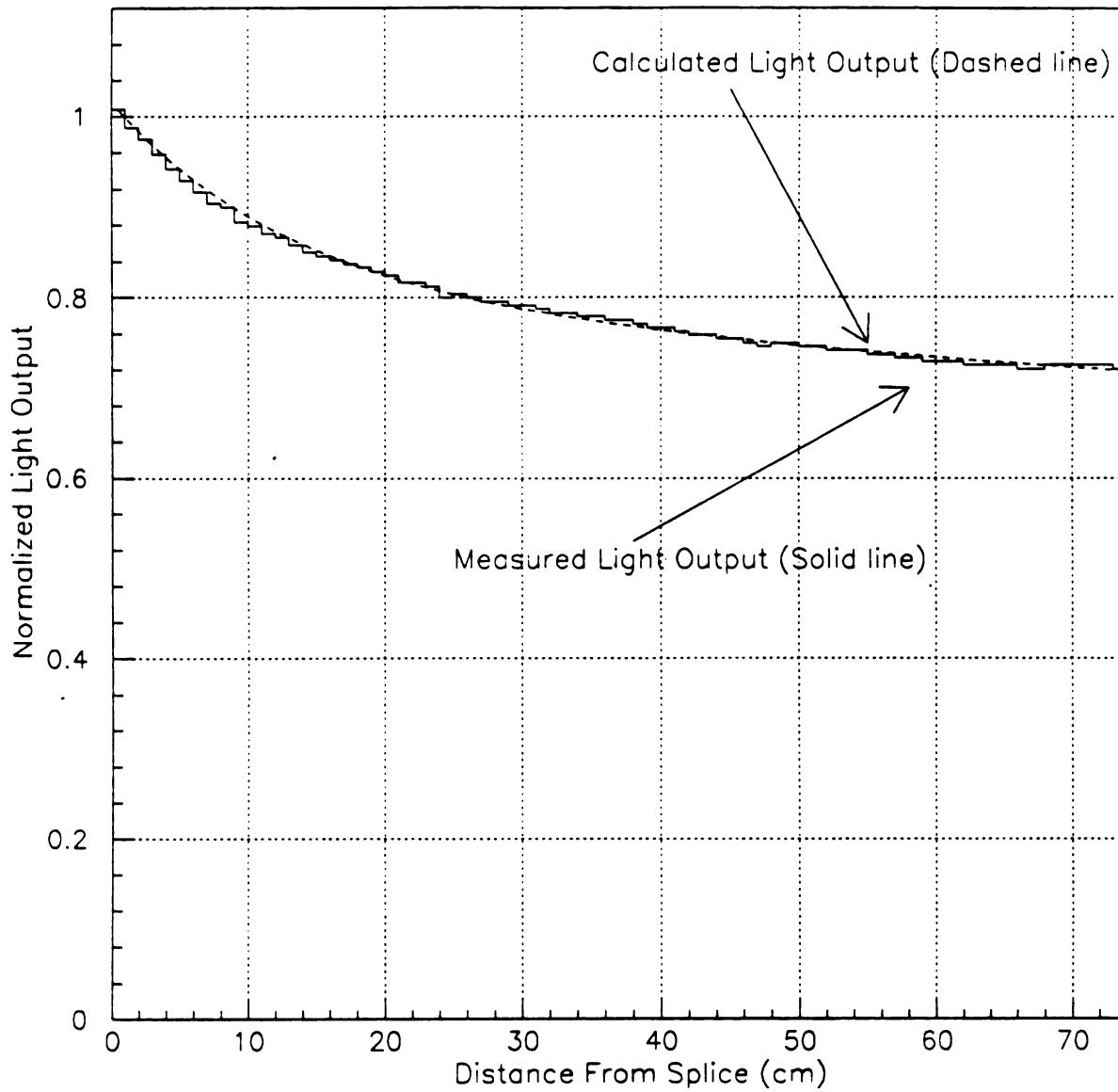


Figure 5.7: Comparison of expected light output and measured light output. The agreement is quite good for the entire length of the fiber.

Date and Time Tested 11/11/83 3:01 PM

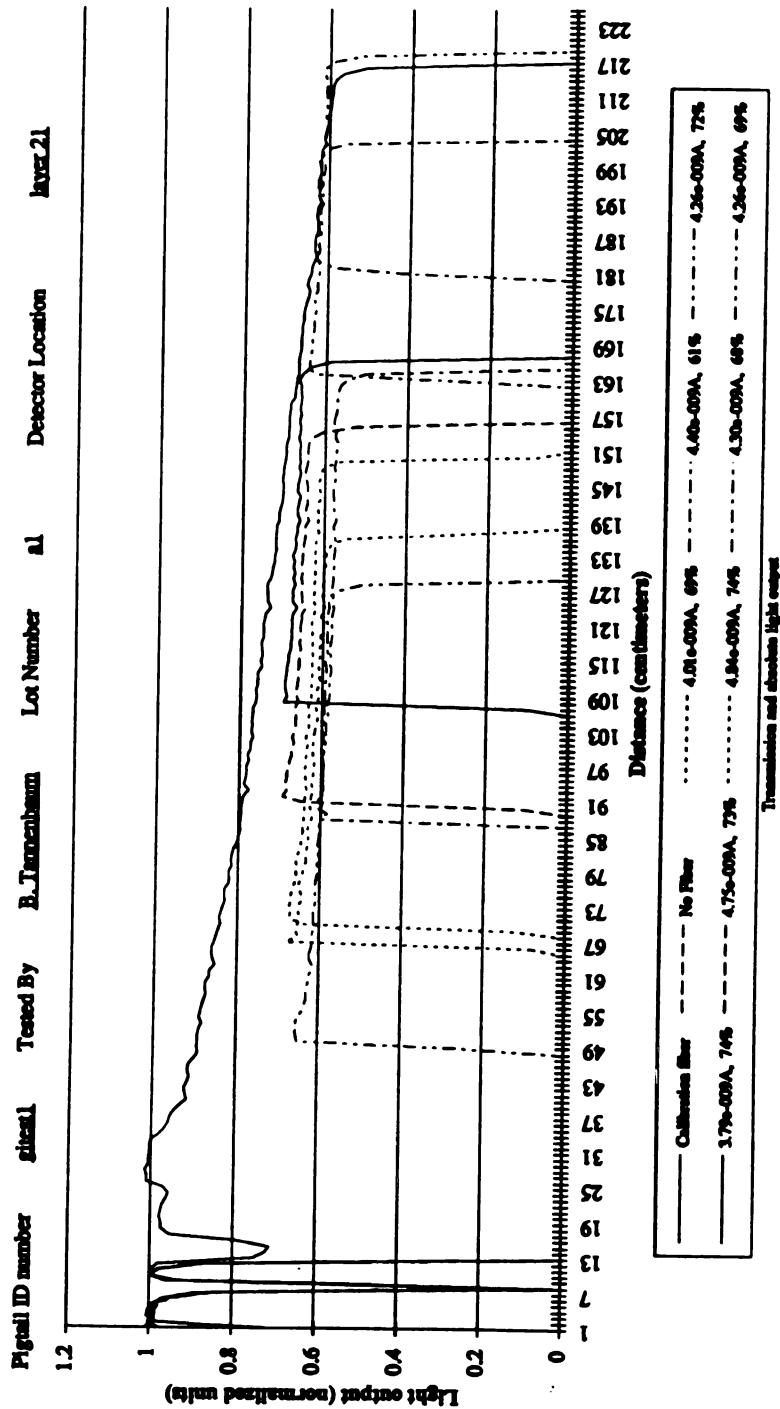


Figure 5.8: Plot of pigtail data taken with multiple fiber linear scanner. The first dip is due to a piece of tape holding the calibration fibers; the second is due to the connector.



the scanner is to measure daily splice quality. Each morning, two fibers are spliced and scanned. The transmission of these fibers is compared with standards to ensure the equipment is producing consistently good splices.

# Chapter 6

## The Splicer: Research and Results

The first tests done on spliced fibers were measurements of their tensile strength, as a relationship between splice quality and the strength of the fiber had previously been noted. A variety of heating times and horizontal pressures were examined. The results for these tests are in Table 6.1. These results were used to narrow the search for the best heating times and pressures.

Initial splicing was done with Bicon BCF91A 0.75 mm $\phi$  fiber. Bicon has a problem maintaining a consistent fiber diameter and only splices moderately well. After a few comparison tests, Kuraray Y11(250) fiber was selected. Initially, a single clad fiber was used, but more experiments showed double clad fiber spliced better and captured more light. A fiber spliced without a sleeve has a minimum bending radius of 15 cm before damage occurs. This is unacceptable in any practical application. Adding an FEP shrink tube over the joint before splicing– the tube is left in place after splicing– decreases the minimum bending radius to 2 cm. The shrink tube is purchased large and shrunk to the proper inner diameter using a heat gun and an appropriately sized gauge pin. Experimentation revealed that a tube larger than the fiber results in large bulges at the splice and poor transmission; a small tube makes assembly difficult and can result in splice failures.

A variety of heating times and horizontal pressures were tried. After finding the best combination for 0.75 mm $\phi$  fiber, the hadron group for the plug upgrade decided to switch to 0.83 mm $\phi$  fibers. After more experimentation, it was determined that 15 seconds of heat and 1.5 psi consistently gave splices with excellent transmission. In late December 1992, as a comprehensive study of the effects of pressure and heating time on splice quality began, a dramatic drop in percent transmission was observed. After much frustration and contact with Kuraray, it was determined that this drop was due to a change in the extrusion process used to make the fiber. The new type of fiber, called S-Type, is more flexible (it has a much smaller bending radius) but conducts 25% less light than does the older type of fiber. The old type, referred to as Non S-Type, splices better and was selected as the fiber of choice for the plug hadron calorimeter upgrade.<sup>1</sup> Table 6.2 is a comparison of various attributes for fibers spliced with the semi-automatic splicer.

The preparation of the ends to be spliced was also examined. Careful end preparation results in both a better average transmission and a smaller sigma. Table 6.3 is a comparison of razor blade polishing versus diamond polishing. The former is done using a brass block with a hole of the proper diameter and a razor blade; the latter is done with a machine designed by engineers at Fermilab and built by AVTech.<sup>2</sup> Any debris left on the ends or in the shrink tube is blown off using compressed nitrogen.

To study the transmission behavior for a large batch of fibers, 100 splices were made. Since these were the first splices made by a new technician, this was also used to determine the learning curve for splicing. The results for this study are in Table 6.4. The technician also attempted to identify which fibers had bad splices and which had

---

<sup>1</sup>The plug electromagnetic calorimeter upgrade group, in Japan, are able to successfully splice S-Type fiber using a very different splicing technique. See Reference [3] for details.

<sup>2</sup>Carl W. Lindenmeyer, John B. Korienek and Masanori Mishina. A paper is to be published in NIM.

good splices. Unfortunately, there was little correlation between appearance of the splice (how much light leaks out at the splice) and the percent transmission across it. Figure 6.1 is a comparison of the good, reasonable, and bad splices. While the bad fibers have some of the lower percent transmissions, many would pass as good splices.

Timing studies were done using this large batch of splices. It was determined that to cut to length, polish and splice a fiber takes 6 minutes. Two minutes of this time is the time for one splicing cycle. This resulted in the need for 4 technicians to produce the fibers so the endplugs will be completed in time for installation prior to Run 2.

These results lead us to believe it is possible to successfully build a calorimeter that will meet the criteria presented in the Introduction. The transmission across the splice is 95.7%, with a variation of 3.7%. This small variation allows for further variation in the tiles, while still meeting the criteria to have tile-to-tile variation of less than 10%. Also, we believe it is possible to construct a quality device in the time allotted.

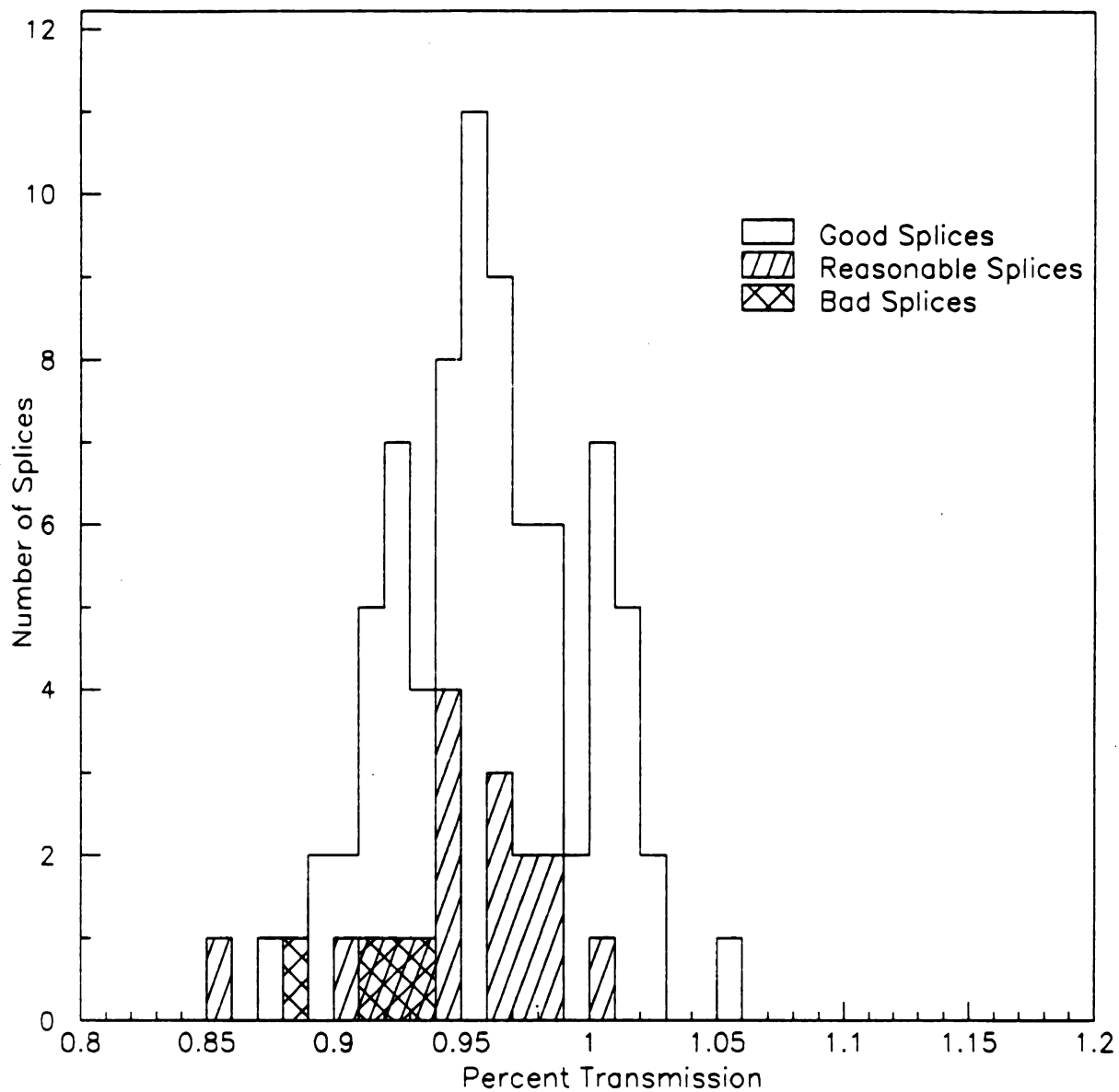


Figure 6.1: Comparison of good, reasonable and bad splices. The bad splices are indeed lower than average, but some of the good splices are equally poor. Many of the fibers were not measured before splicing and used a standard fiber for normalization. This results in a few splices with apparent transmission over 100%.

Table 6.1: Tensile Strength: Kuraray versus Bicon. A long heating time and high pressure make stronger splices. The apparent greater strength of the Bicon fiber is due to the mismatch in sizes for the Kuraray fiber (no clear Kuraray of the proper size was available during this test).

Pressure (psi)	Heating Time (seconds)	Breaking Pressure (pounds)
Kuraray Y11(250) 0.75 mm $\phi$ to Kuraray clear 0.83 mm $\phi$		
1.5	20	3.30
1.5	10	5.65
1.2	10	4.30
1.2	7	3.30
1.0	10	3.75
1.0	7	3.00
0.8	10	3.60
0.6	15	3.95
0.6	10	1.50
Bicon 0.75 mm $\phi$ to Bicon clear 0.75 mm $\phi$		
1.5	15	6.45
1.5	10	6.45
1.2	10	6.30
1.2	7	2.70
1.0	15	6.25
0.8	15	2.65
0.6	20	2.75
0.6	10	2.70

Table 6.2: Comparison of Kuraray Y11(250) Non-S and S type fibers. The only property in which the S type fiber excels is in bending radius. For our application, this was secondary to light transmission and Non-S type was chosen.

Fiber	Sample Size	Transmission %	$\frac{\sigma}{\text{Mean}}$	Bending Radius (cm)	Normalized Light Transmission
S Type	15	82.6	6.0	.5	0.75
Non-S Type	13	94.2	1.7	2	1.0

Table 6.3: Fiber End Preparation: Razor Blade versus Diamond Polisher. The Diamond Polisher significantly improves the splice quality and adds only 2 minutes of preparation time per splice.

End Preparation	Sample Size	Transmission %	$\frac{\sigma}{\text{Mean}}$
Razor Blade	20	91.9	5.2
Diamond Polisher	19	95.1	3.0

Table 6.4: Study of a large batch of spliced fibers. After a 40 fiber learning curve, the quality of the splice improves. While the bad splices seem worse than the good, some of the worst splices are in the good group.

Sample	Transmission (%)	$\frac{\sigma}{\text{Mean}}$
All 100 fibers	95.7	3.7
First 40 fibers	94.0	3.9
Last 60 fibers	96.8	3.9
79 "good" fibers	96.0	3.8
17 "ok" fibers	94.9	3.7
4 "bad" fibers	91.7	2.0

# Chapter 7

## XY Scanners: Photomultiplier Response Uniformity

The completed endplug calorimeter will use over 2000 photomultiplier tubes. Also, the surface of the photomultiplier must have a uniform response over the entire surface. To ensure this uniformity, a light mixer is fixed to the face of the photomultiplier. Thus, instead of light from the fibers entering the photomultiplier directly, it must pass through the light mixer. This removes any position dependence for the photomultiplier response.[5,6]

To investigate the surface response uniformity, an *x-y* scanner was constructed. It consists of a green LED attached to two 1 mm $\phi$  clear fibers. One of these fibers leads to a fixed phototube; it is used to calibrate of the light output of the LED. The other fiber is placed in a mount aimed at the phototube to be scanned (Figure 7.1). The LED can moved over an area of 28 by 28 cm<sup>2</sup>. The entire LED assembly is attached to rollers controlled using an IBM PC. The phototubes are read out through CAMAC. The current PC-based software allows the user to scan the entire surface of a 1 inch diameter phototube, in 1mm steps, in 15 minutes. Larger tubes can be scanned in correspondingly longer times.

Two different modes exist for the *x-y* scanner. In the first mode, an 8 mm long



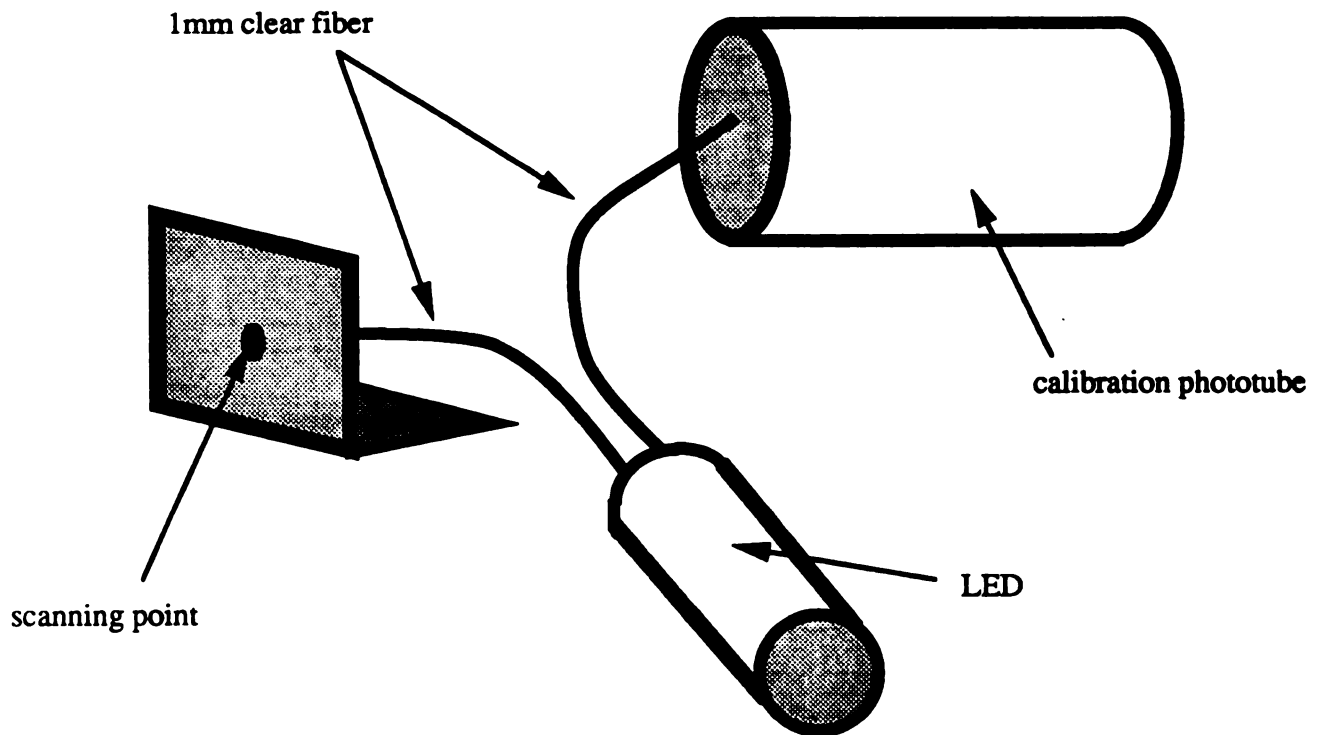


Figure 7.1: Detail of the *x-y* scanner. Light from the LED passes through the 1 mm $\phi$  clear fiber to the calibration tube and to scanning point. The scanner has 1 mm resolution.

by 1 mm $\phi$  tube is placed over the end of the clear fiber. The inside of this tube is painted black and the tube acts as a collimator. Light from the end of the fiber diverges in a cone with half-angle 22°. By placing the collimator over the end of the fiber, the angle of divergence is reduced to 11°. If the face of the photomultiplier is placed within 1-2 mm of the end of the tube, the light reaching the photocathode is a circle of diameter 2 mm (Figure 7.2). Scans made with the collimator in place will be accurate for scans of position versus output and are useful in examining photocathode response uniformity. However, light leaving a fiber *does* diverge in a 22° cone. Thus, for light mixer studies, the collimator must be removed. If it is not removed, the light does not sufficiently diverge and renders the light mixer useless.

To determine the effectiveness of a light mixer, four scans are made. First, a scan of the phototube, using the collimator is made (Figure 7.3). This allows the user to see if the phototube is acceptably uniform for this type of study— there are limits on how well even the best light mixer will perform. Next, a small, black, opaque dot is placed on the surface of the photomultiplier and the tube is again scanned with the collimator in place. The next scan is done with both the light mixer and dot in place. The collimator is removed so the light mixer can function. In the final scan, the dot is removed and the tube is scanned with just the light mixer. For the plots shown, the tube used was a Hamamatsu R4125, which has a 1.5 cm diameter photocathode. The dot used with this tube had a diameter of 5 mm. By placing the dot on the photocathode, a defect is created. If the light mixer can remove this defect, than it is an effective light mixer. As can be seen in Figure 7.4, the defect is indeed removed. The only effect of the dot is to lower the overall response of the tube by 5%. Since the dot effectively decreases the active area of the photocathode by  $0.5^2/1.5^2 = 0.11$ , this loss is expected (the loss is less than expected as the dot only reduces the light by  $\approx 50\%$ ). For this test, the light mixer used was 40 mm long, and the side placed

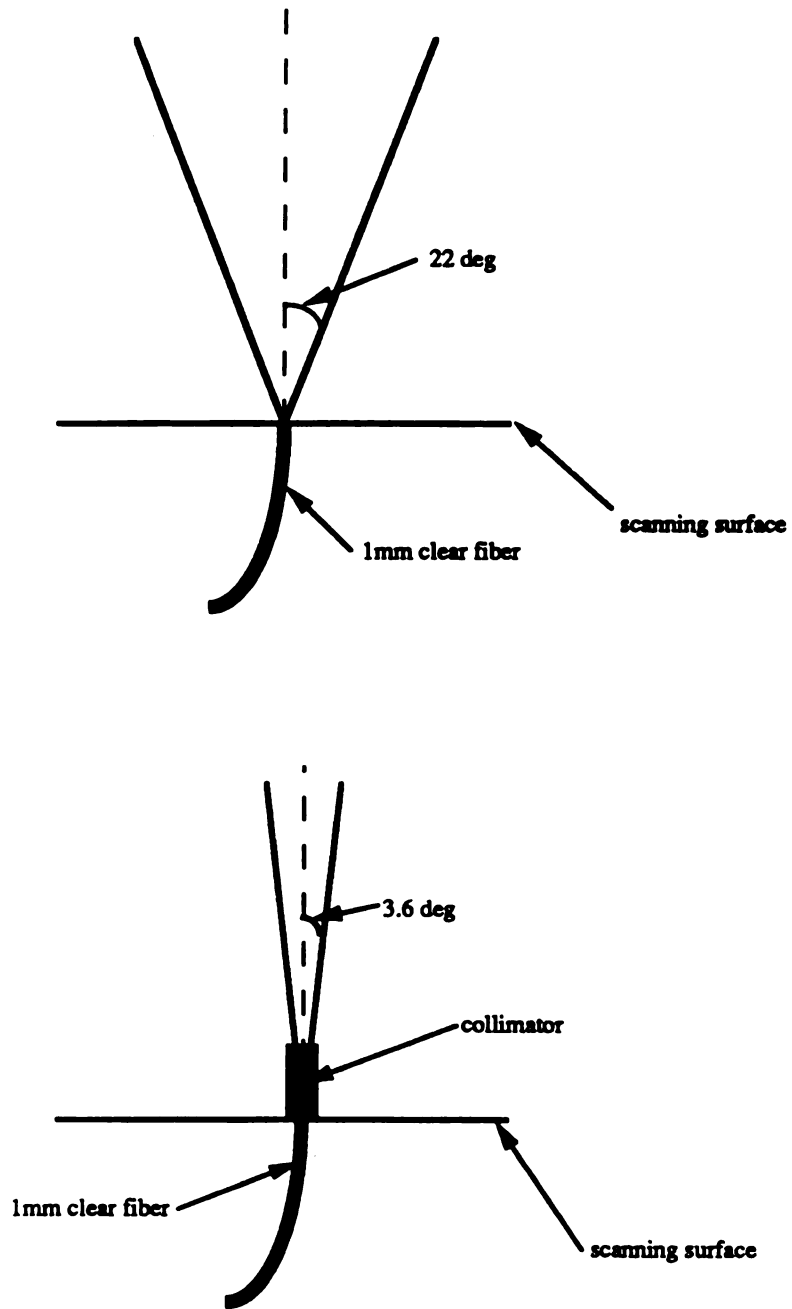


Figure 7.2: The collimator is used when determining the uniformity. However, when studying light mixers, it must be removed. Light from a real fiber will not be collimated and collimated light cannot be mixed.

on the photomultiplier was a square 10 mm on a side. As can be seen in Figure 7.4, an area of roughly 100 mm<sup>2</sup> has the same response (to within 5%).

The *x-y* scanner is an effective device for testing both light mixers and photomultipliers. Further tests are underway to examine a variety of differently shaped and sized light mixers. Also, the plug upgrade PMT group plans to scan a fraction of the incoming photomultiplier tubes as a quality control.

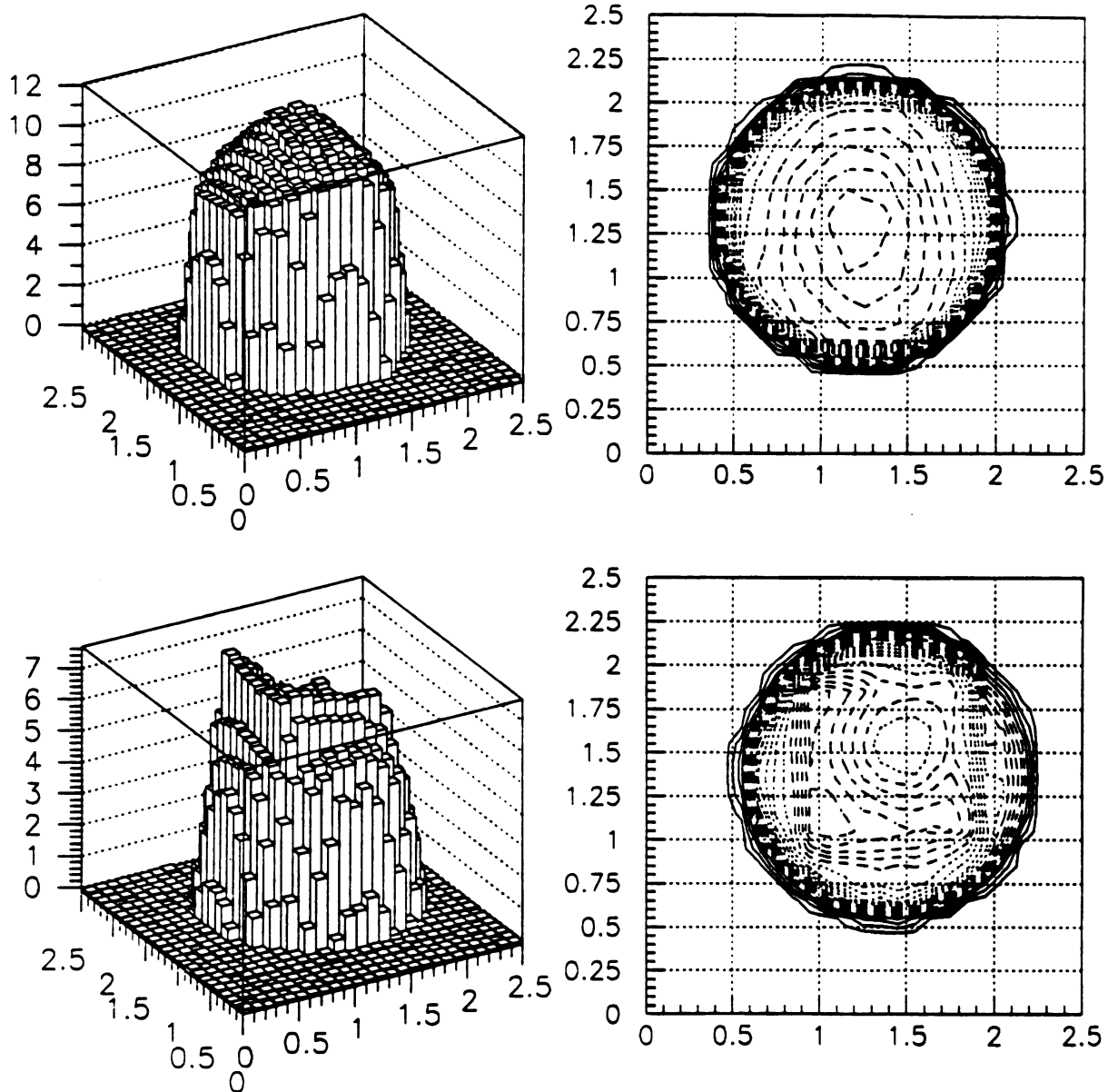


Figure 7.3: The upper plot is a scan of a bare photomultiplier using the collimator. The lower plot is a scan of the same photomultiplier with a 40 mm light mixer, the collimator, and a 5 mm $\phi$  black dot placed in one corner. Each line on the contour plot is 5%.

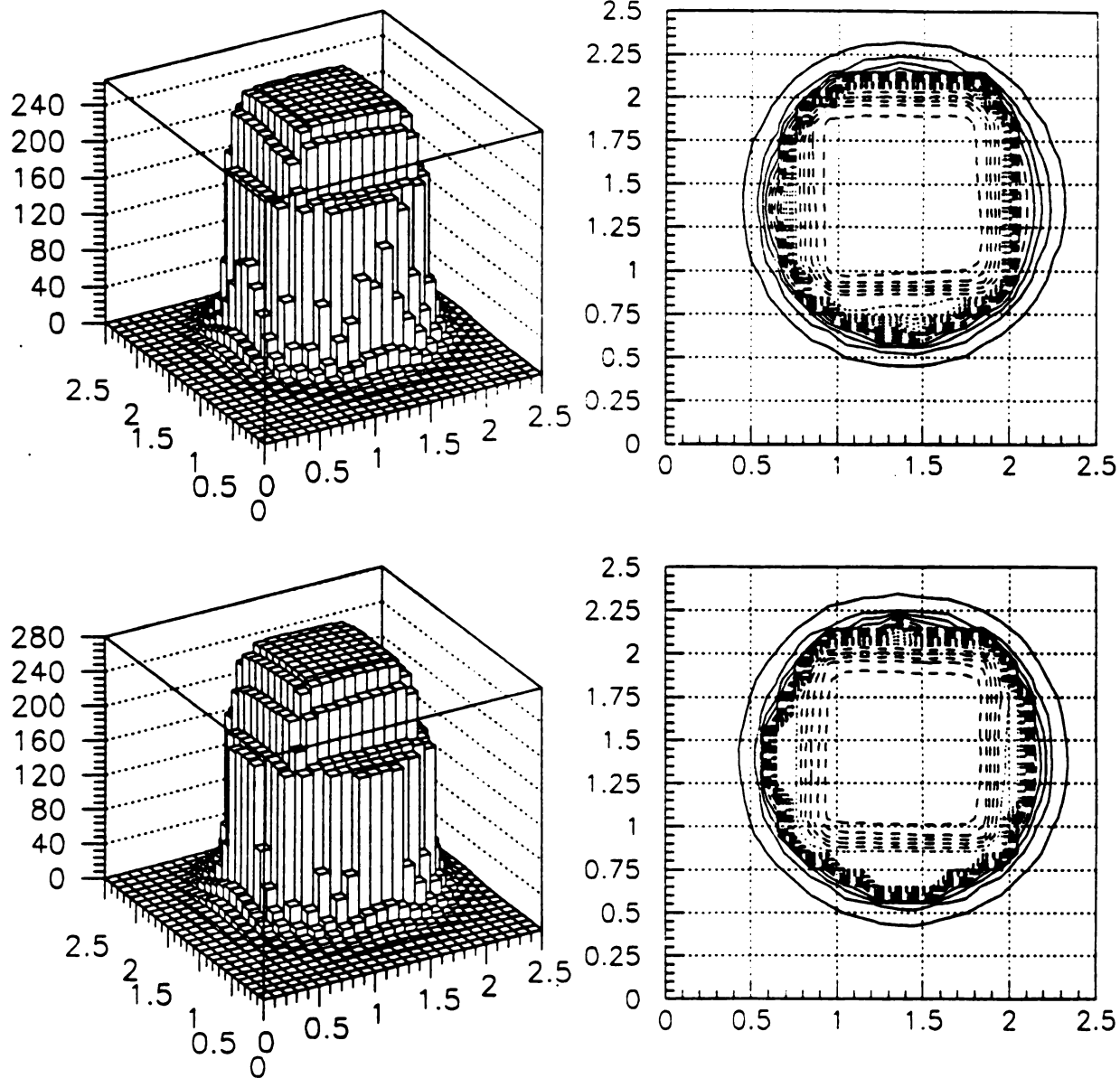


Figure 7.4: Both plots are with a 40 mm light mixer but without the collimator. The upper plot is with the dot; the lower is without it. The light mixer effectively mixes the light and removes the effect of the dot, with a 4% reduction in output. Each line on the contour plot is 5%.

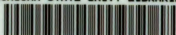
# Bibliography

# Bibliography

- [1] Deninno, M. *et. al.* CDF Plug Upgrade Draft 1.
- [2] M. Atac, W. Foster, M. Lundin, "A Simple Method for Fusing Plastic Fibers", Fermilab technical note FN-537, March 1990.
- [3] C. Bromberg, J. Huston, R. Miller, S. Pollack, D. Shooltz, K. Tollefson, B. Williams, "A Dichromatic Scintillating Fiber Calorimeter", Proceedings of the Calorimetry Conference, 1990.
- [4] Hara, K., Horiuchi, K., Kim, S., Takikawa, K., Yasouka, K., Koyano, M., Matsui, S., Okumura, H, "Heat Splicing of Plastic Fibers Using PEEK Tube". CDF/DOC/PLUG\_UPGR/CDFR/1950, February 5, 1993.
- [5] Koksa, Wayne, "Light Mixer Study", Fermilab technical note TS-DET 93-038, June 1993.
- [6] Koksa, Wayne, "Photocathode Scans of Hamamatsu R4125 PMTs", Fermilab technical note TS-DET 93-045, June 1993.



MICHIGAN STATE UNIV. LIBRARIES



31293010269730